

Effect of the bound nucleon form factors on charged-current neutrino-nucleus scattering

K. Tsushima¹ *, Hungchong Kim² †, and K. Saito³ ‡

¹Department of Physics and Astronomy, University of Georgia, Athens, Georgia 30602, USA

²Institute of Physics and Applied Physics, Yonsei University, Seoul, 120-749, Korea

³Tohoku College of Pharmacy, Sendai 981-8558, Japan

Abstract

We study the effect of bound nucleon form factors on charged-current neutrino-nucleus scattering. The bound nucleon form factors associated with the vector and axial-vector currents are calculated in the quark-meson coupling model. We compute the inclusive $^{12}\text{C}(\nu_\mu, \mu^-)X$ differential and total cross sections, which have been measured by the LSND collaboration at Los Alamos, using a relativistic Fermi gas model with the calculated bound nucleon form factors. It is shown that the bound nucleon form factors reduce the total cross section by about 8% relative to that calculated with the free nucleon form factors, where most of the conventional calculations overestimate the total cross section data by about 30% to 100%. The present correction is important because the cross section serves as a crucial input in the determination of fundamental parameters, particularly those related with the neutrino oscillations.

PACS: 24.85+p; 25.30.Pt; 71.10.Ca; 21.65.+f

Keywords: Bound nucleon form factors, Neutrino-nucleus scattering, Relativistic Fermi gas model, Quark-meson coupling model

*tsushima@physast.uga.edu

†hung@phya.yonsei.ac.kr

‡ksaito@tohoku-pharm.ac.jp

1 Introduction

There has been of considerable interest in possible changes in the bound nucleon properties in nuclear medium [1]. A number of evidences, such as the variation of nucleon structure functions in lepton deep-inelastic scattering off nuclei (the nuclear EMC effect) [2], the quenching [3, 4] (enhancing) [5] of the space (time) component of the effective one-body axial coupling constant in nuclear β decays, the missing strength of the response functions in nuclear inelastic electron scattering and the suppression of the Coulomb sum rule [6], have stimulated investigations of whether or not the quark degrees of freedom play any vital role.

Recently, the electromagnetic form factors of bound protons were studied in polarized $(\vec{e}, e'\vec{p})$ scattering experiments on ^{16}O [7] and ^4He [8]. In the experiments at MAMI and Jefferson Lab on ^4He [8], the measured ratio of the transverse to longitudinal polarizations, which is directly proportional to the ratio of the electric (G_E^p) to magnetic (G_M^p) Sachs proton form factors, was found to differ by about 10% in ^4He from that in ^1H . Conventional models employing free proton form factors, phenomenological optical potentials, and bound state wave functions, as well as relativistic corrections, meson exchange currents (MEC), isobar contributions and final state interactions (FSI) [7, 8, 9], fail to account for the observed effect in ^4He [8]. Indeed, full agreement with the data was obtained only when, in addition to these standard nuclear structure corrections, a small correction due to the internal structure of the bound proton was taken into account [7, 8, 10].

As for the electro-weak vector and axial-vector form factors of bound nucleons, it is essential to have a good knowledge of them for the precise estimates of the neutrino-nucleus cross section. The cross section serves as a crucial input in the determination of fundamental parameters, particularly those related with the neutrino oscillations [11]. It is also a key ingredient in neutrino astrophysics [12] and in the investigations of strangeness in nucleon [13]. Thus, it is important to estimate the neutrino-nucleus cross section as precise as possible, including all corrections such as from the bound nucleon form factors, in order to give tighter constraints on the fundamental parameters.

In this article we study the effect of the bound nucleon form factors on neutrino-nucleus scattering ¹. We compute the inclusive $^{12}\text{C}(\nu_\mu, \mu^-)X$ differential and total cross sections that have been measured by the LSND collaboration [14] at Los Alamos. It is known that the existing calculations for the total cross section based on the nucleon and meson degrees of freedom overestimate the data by about 30% to 100% [14, 15]. Because we want to focus on the effects due to the internal structure change of the bound nucleon, we use a relativistic Fermi gas model [16, 17], which is simple and transparent for the purpose, while implementing the bound nucleon form factors calculated in the quark-meson coupling (QMC) model [10, 18]. Thus, we do not here include the other nuclear structure corrections [15, 19], such as Δ -hole excitations, MEC, FSI etc.

Of course, one must keep in mind that it is difficult to separate the effects we consider here from the standard nuclear-structure corrections, particularly from MEC. However, since the relevant current operators in the present study are one-body quark (pion) operators acting on the quarks (pion cloud) in the nucleon, a double counting with the model-dependent MEC,

¹Because the renormalization of axial-vector form factors are the same for the time and space components in the present study (quenched), we will not discuss issues concerning the enhancement of the time component (axial charge) due to MEC.

in which the current operators act on the mesons being exchanged [4, 20], is expected to be avoided. The same is also true for the model-independent meson pair currents, because they are based on the *anti-nucleon* degrees of freedom, although the current operators act on one of the two interacting-nucleons [3, 4, 20]. For the vector current, a possible double counting with MEC is practically avoided as the analyses for the ${}^4\text{He}(\vec{e}, e'\vec{p}){}^3\text{H}$ experiments [8] have shown. In addition, the MEC contribution to the quasi-elastic electron scatterings appears to give corrections primarily to the nucleon momentum distribution, rather than to the effective electromagnetic form factors of the nucleon [21]. For the axial-vector current, the renormalization of the axial coupling constant ($g_A = G_A(0)$) due to the model-independent meson pair currents, which may be nontrivial to disentangle from the correction we focus on, was estimated [4] using a Fermi gas model. The renormalization of g_A due to the model-independent meson pair currents, amounts to give a 2% quenching at normal nuclear matter density thus contributing negligibly to the cross section. Hence, the interference between the axial-vector and vector currents is also expected not to suffer from the double counting, when considered together with the analyses for the ${}^4\text{He}(\vec{e}, e'\vec{p}){}^3\text{H}$ experiments. Thus, the effect we consider here, which originates from the change of the internal quark wave function at the mean-field level, should be taken into account additionally to the standard nuclear corrections.

2 Quark-meson coupling model

The QMC model [22] has been successfully applied to many problems of nuclear physics and hadronic properties in nuclear medium [23]. In the model, the medium effects arise through the self-consistent coupling of scalar (σ) and vector (ω) meson fields to confined quarks, rather than to the nucleons. As a result, the internal structure of the bound nucleon is modified by the surrounding nuclear medium. The nucleon is usually described by the MIT bag model [24, 25]. The Lagrangian density of the QMC model for symmetric nuclear matter is thus given by [22]

$$\mathcal{L}_{\text{QMC}} = [\bar{\psi}_q(i\gamma^\mu\partial_\mu + g_\sigma^q\sigma - g_\omega^q\gamma^\mu\omega_\mu - m_q)\psi_q - B]\theta_v - \frac{1}{2}\bar{\psi}_q\psi_q\delta_s + \mathcal{L}_M, \quad (1)$$

where ψ_q is the light quark field ($q = u$ and d), B is the bag constant and g_σ^q (g_ω^q) is the quark- σ (ω) meson coupling constant. θ_v is a step function equal to unity inside the confining volume and vanishing outside, and δ_s is the surface δ -function. We assume SU(2) symmetry for the u and d quarks, and use the current quark mass, $m_q = 5$ MeV. \mathcal{L}_M describes the kinetic and mass terms for the meson fields in free space.

In the mean field approximation, the quark field inside the bag satisfies the Dirac equation

$$\left[i\gamma^\mu\partial_\mu - (m_q - g_\sigma^q\bar{\sigma}) - g_\omega^q\bar{\omega}\gamma^0 \right] \psi_q(x) = 0, \quad (2)$$

where $\bar{\sigma}$ and $\bar{\omega}$ denote respectively the constant mean values of the scalar and the time component of the vector field in symmetric nuclear matter. Hereafter we denote the in-medium quantities, or bound nucleon quantities, by an asterisk *.

In the present calculation, we fix the bag parameters so as to produce the free nucleon mass, $m_N (= 939 \text{ MeV})$, and the nucleon bag radius, $R_N = 0.8 \text{ fm}$. Furthermore, the quark-meson coupling constants are determined by fitting the nuclear saturation property (the average binding energy per nucleon is 15.7 MeV) at normal nuclear matter density ($\rho_0 = 0.15 \text{ fm}^{-3}$).

All values of the bag parameters and coupling constants can be found in Ref. [22]. One of notable features is that the calculated incompressibility, $K \simeq 280$ MeV, is well within the experimental range, $K_{exp} = 200 - 300$ MeV. Although the bag radius shrinks a little at finite nuclear density ρ_B , the root-mean-square radius of the quark wave function actually increases by a few percent at nuclear saturation density, which relates to the modification of in-medium form factors discussed in the next section.

3 In-medium form factors

Assuming G-parity (no second-class current), the charged-current vector and axial form factors are defined by

$$\langle p' s' | V_a^\mu(0) | p s \rangle = \bar{u}_{s'}(p') \left[F_1(Q^2) \gamma^\mu + i \frac{F_2(Q^2)}{2m_N} \sigma^{\mu\nu} (p' - p)_\nu \right] \frac{\tau_a}{2} u_s(p), \quad (3)$$

$$\langle p' s' | A_a^\mu(0) | p s \rangle = \bar{u}_{s'}(p') \left[G_A(Q^2) \gamma^\mu + \frac{G_P(Q^2)}{2m_N} (p' - p)^\mu \right] \gamma_5 \frac{\tau_a}{2} u_s(p), \quad (4)$$

where $Q^2 \equiv -(p' - p)^2$, and τ_a and $u_s(p)$ are the Pauli matrices and nucleon Dirac spinor, respectively. The vector form factors, $F_1(Q^2)$ and $F_2(Q^2)$, are related to the electric ($G_E(Q^2)$) and magnetic ($G_M(Q^2)$) Sachs form factors by the conserved vector current hypothesis. The induced pseudoscalar form factor, $G_P(Q^2)$ in Eq. (4), is dominated by the pion pole and can be calculated using the PCAC relation. Nevertheless, the contribution from $G_P(Q^2)$ to the cross section is proportional to (lepton mass) $^2/m_N^2$, which is small in the present study involving muon.

Using the improved cloudy bag model (ICBM) [26] with QMC, the electromagnetic and axial form factors in nuclear medium are calculated in the Breit frame [10, 18]

$$G_{E,M,A}^{QMC*}(Q^2) = \eta^2 G_{E,M,A}^{sph*}(\eta^2 Q^2), \quad (5)$$

where the scaling factor is $\eta = (m_N^*/E_N^*)$, with $E_N^* = \sqrt{m_N^{*2} + Q^2/4}$ the energy, and m_N^* the effective mass of the nucleon in nuclear medium. The ICBM includes a Peierls-Thouless projection to account for center of mass and recoil corrections, and a Lorentz contraction of the internal quark wave function [26, 27]. The scaling factor η in the argument of $G_{E,M,A}^{sph*}$ arises from the coordinate transformation of the struck quark, and the prefactor in Eq. (5) comes from the reduction of the integral measure of the two spectator quarks in the Breit frame. $G_{E,M,A}^{sph*}$ are the form factors calculated with the static spherical bag wave function

$$G_E^{sph*}(Q^2) = \frac{1}{D} \int d^3r j_0(Qr) f_q(r) K(r), \quad (6)$$

$$G_M^{sph*}(Q^2) = \frac{1}{D} \frac{2M_N^*}{Q} \int d^3r j_1(Qr) \beta_q^* j_0(x_q r/R_N^*) j_1(x_q r/R_N^*) K(r), \quad (7)$$

$$G_A^{sph*}(Q^2) = \frac{5}{3} \int d^3r \{ [j_0^2(x_q r/R_N^*) - \beta_q^{*2} j_1^2(x_q r/R_N^*)] j_0(Qr) + 2\beta_q^{*2} j_1^2(x_q r/R_N^*) [j_1(Qr)/Qr] \} K(r)/D. \quad (8)$$

In Eqs. (6)–(8), $f_q(r) = j_0^2(x_q r/R_N^*) + \beta_q^{*2} j_1^2(x_q r/R_N^*)$, where R_N^* is the nucleon bag radius in medium, x_q the lowest eigenfrequency, and $\beta_q^{*2} = (\Omega_q^* - m_q^* R_N^*)/(\Omega_q^* + m_q^* R_N^*)$, with $\Omega_q^* = \sqrt{x_q^2 + (m_q^* R_N^*)^2}$ and $m_q^* = m_q - g_\sigma^* \bar{\sigma}$. The recoil function $K(r) = \int d^3x f_q(\vec{x}) f_q(-\vec{x} - \vec{r})$ accounts for the correlation of the two spectator quarks, and $D = \int d^3r f_q(r) K(r)$ is the normalization factor.

Now we calculate ratios of the bound to free nucleon form factors, $G_{E,M,A}^{QMC^*}/G_{E,M,A}^{ICBM\ free}$, to estimate the bound nucleon form factors $G_{E,M,A}^*$. Using the empirical parameterizations in free space, $G_{E,M,A}^{emp}$ [28, 29], the bound nucleon form factors $G_{E,M,A}^*$ are given by

$$G_{E,M,A}^*(Q^2) = \left[\frac{G_{E,M,A}^{QMC^*}(Q^2)}{G_{E,M,A}^{ICBM\ free}(Q^2)} \right] G_{E,M,A}^{emp}(Q^2). \quad (9)$$

Note that the pion cloud effect is not included in the axial form factor in the present treatment [18]. However, the normalized Q^2 dependence, which is divided by $g_A = G_A(0)$, relatively well reproduces the empirical parameterization [18]. Furthermore, the relative modification of $G_A^*(Q^2)$ due to the pion cloud is expected to be small, since the pion cloud contribution to entire g_A is about 8 % [24] without a specific center-of-mass correction.

Fig. 1 shows the ratios of the bound to free nucleon form factors as a function of Q^2 for $\rho_B = \rho_0$ and $0.668\rho_0$ (corresponding to the Fermi momentum $k_F = 225$ MeV for ^{12}C). The lower panels in Fig. 1 show the enhancement of momentum dependence of $F_2^*(Q^2)$ and $G_A^*(Q^2)$, as well as the enhancement of $F_2^*(0)$ and quenching of $G_A^*(0)$ [10, 18, 30]. Although the modification of the Q^2 dependence is small, we emphasize that this is a very interesting effect originating from the nucleon internal structure change. The main origin of this new Q^2 dependence is the Lorentz contraction effect to the quark wave function amplified by the reduction in the effective nucleon mass. (See Eq. (5).)

We here note that in the QMC model the relative change of the proton electric form factor to the free one in matter ($G_E^{p^*}/G_E^p$) at normal nuclear density is only about 4 % at moderate momentum transfer (e.g. $Q^2 = 0.15$ GeV²). For the magnetic form factor, the change is much less (at most 1 %). The amount of these changes is consistent with the constraints derived from the y-scaling analysis in quasi-elastic inclusive electron-nucleus scattering data [31].

4 Numerical results for neutrino-nucleus cross sections

We compute the charged-current $^{12}\text{C}(\nu_\mu, \mu^-)X$ differential and total cross sections, which have been measured by the LSND collaboration [14]. We use the formalism described in Ref. [16], and the empirical parameterizations of the electromagnetic [16, 28] and axial [18, 29] form factors for the free nucleon. (See Eq. (9).) A relativistic Fermi gas model, which is simple and thus transparent to see how the bound nucleon form factors affect the cross section, is used to calculate the differential cross section $\langle d\sigma/dE_\mu \rangle$, averaged over the LSND muon neutrino spectrum $\Phi(E_{\nu_\mu})$ [16]

$$\left\langle \frac{d\sigma}{dE_\mu} \right\rangle = \frac{\int_0^\infty (d\sigma/dE_\mu) \Phi(E_{\nu_\mu}) dE_{\nu_\mu}}{\int_0^\infty \Phi(E_{\nu_\mu}) dE_{\nu_\mu}}. \quad (10)$$

Here, the integrations have been carried out using the full range of the LSND experimental spectrum [14], $0 \leq E_{\nu_\mu} \leq 300$ MeV.

Fig. 2 shows the result of $\langle d\sigma/dE_\mu \rangle$ calculated using the free nucleon mass as well as the effective nucleon mass m_N^* . We use the Fermi momentum $k_F = 225$ MeV, which corresponds to ^{12}C , and $m_N^* = 802.8$ MeV (the mass at $\rho_B = 0.668\rho_0$) obtained in the QMC model. A moderate quenching of the cross section can be observed due to the in-medium form factors for both cases. Although the effective nucleon mass can account for, to some extent, the binding effect (the Hugenholtz-van Hove theorem) [32], there is an alternative to include the binding effect, i.e., the “binding energy” E_B is introduced and the available reaction energy E is replaced by $E - E_B$. In this case, we use the free nucleon mass in the calculation. Since E_B is an effective way of accounting for the binding effect [33], we regard E_B as a parameter and perform calculations for $E_B = 20, 25$ and 30 MeV. (For example, $E_B = 25 - 27$ MeV is commonly used for the ^{16}O nucleus [34].) We emphasize that our aim is not to reproduce the LSND data, but to estimate the corrections due to the bound nucleon form factors. In Fig. 3 we present the results of $\langle d\sigma/dE_\mu \rangle$ for $E_B = 20, 25$ and 30 MeV. In both figures 2 and 3, the bound nucleon form factors certainly reduce the differential cross section. In Fig. 3, as the binding energy E_B increases, the peak position shifts downward for both cases with the free and bound nucleon form factors. The similar tendency due to the effective nucleon mass m_N^* is also seen in Fig. 2.

The total cross section is given by integrating Eq. (10) over the muon energy. We denote the cross section calculated with the free nucleon form factors, $F_{1,2}(Q^2)$ and $G_{A,P}(Q^2)$, as $\langle \sigma(F, G) \rangle$, and that obtained with the bound nucleon form factors, $F_{1,2}^*(Q^2)$ and $G_{A,P}^*(Q^2)$, as $\langle \sigma(F^*, G^*) \rangle$. Thus, $\langle \sigma(F, G) \rangle$ calculated with m_N and $E_B = 0$ corresponds to the free Fermi gas model result. The results with $E_B = 0$ and either m_N or m_N^* are listed in the top group rows in Table 1. The LSND experimental data [14] are also shown in the bottom group rows in Table 1. As expected [14], the free Fermi gas result overestimates the data by a factor of three. The results obtained using the bound nucleon form factors, with either m_N or m_N^* , similarly overestimate the LSND data. In order to make discussions more quantitative, we define

$$R(\delta\sigma) \equiv \frac{\langle \sigma(F, G) \rangle - \langle \sigma(F^*, G^*) \rangle}{\langle \sigma(F, G) \rangle}. \quad (11)$$

For the total cross sections calculated with (m_N, m_N^*) and $E_B = 0$, we get $R(\delta\sigma) = (7.7, 7.7)\%$, respectively. Thus, the correction due to the bound nucleon form factors to the total cross section is not sensitive to m_N or m_N^* in the case of $E_B = 0$.

Next, we investigate which bound nucleon form factor gives dominant corrections to the total cross section. We calculate the total cross section with m_N using the free and bound nucleon form factors, i.e., $[F_{1,2}^*(Q^2)$ and $G_{A,P}(Q^2)]$ or $[F_{1,2}(Q^2)$ and $G_{A,P}^*(Q^2)]$. They are denoted by $\langle \sigma(F^*, G) \rangle$ and $\langle \sigma(F, G^*) \rangle$, respectively, and the results are given in the middle group rows in Table 1. Then, together with the results in the upper group rows in Table 1, we obtain inequalities for the total cross sections calculated with m_N and $E_B = 0$

$$\langle \sigma(F, G^*) \rangle < \langle \sigma(F^*, G^*) \rangle < \langle \sigma(F, G) \rangle < \langle \sigma(F^*, G) \rangle. \quad (12)$$

This shows that the most dominant reduction is driven by the axial form factor, $G_A^*(Q^2)$. (The induced pseudoscalar form factor $G_P(Q^2)$ gives only a few percent contribution to the total cross section when calculated using all free form factors.) Furthermore, $F_{1,2}^*(Q^2)$ enhance the total cross section (mostly due to $F_2^*(Q^2)$) as can be seen from the lower panel in Fig. 1.

The total cross sections for $E_B = 20, 25$ and 30 MeV are listed in the bottom group rows in Table 1. As discussed for the results with $E_B = 0$, the bound nucleon form factors reduces the total cross section relative to that calculated with the free form factors. In addition, one can notice that the results are rather sensitive to the values for E_B . In these cases, we find $R(\delta\sigma) = (8.1, 7.6, 7.5)\%$ for $E_B = (20, 25, 30)$ MeV, respectively. Thus, the effect of the bound nucleon form factors to the reduction rate is again not sensitive to E_B .

5 Summary

We have estimated the effect of the bound nucleon form factors arising from the nucleon internal structure change on the $^{12}\text{C}(\nu_\mu, \mu^-)X$ differential and total cross sections, that have been measured by the LSND collaboration [14] at Los Alamos. We have used a relativistic Fermi gas model implementing the bound nucleon form factors calculated in the QMC model. The effect of the bound nucleon form factors is a reduction of about 8 % for the total cross section. This 8 % reduction (or an order of 10 % for a heavier nucleus) should be taken into account additionally to the standard nuclear structure corrections. To draw a more definite conclusion, it is essential to perform a more precise, complicated calculation within the framework of RPA [16] including the effect of bound nucleon form factors. Such a calculation should be done in the future. However, even at the present stage, it is important to point out that the correction due to the in-medium form factors could be significant for a precise estimate of the charged-current neutrino-nucleus cross section, in particular, to give tighter constraints for the fundamental parameters associated with the neutrino oscillations.

Acknowledgments

We would like to thank D.H. Lu concerning the improved cloudy bag model codes used to calculate the bound nucleon form factors. Our thanks also go to K. Kubodera, K. Nakayama, and R. Seki for useful discussions. K.T. is supported by the Forschungszentrum-Jülich, contract No. 41445282 (COSY-058).

References

- [1] G.E. Brown, M. Rho, Phys. Rev. Lett. 66, 2720 (1991);
P.A.M. Guichon, Nucl. Phys. A 680, 229c (2001)
- [2] M. Arneodo, Phys. Rep. 240, 301 (1994);
D.F. Geesaman, K. Saito, A.W. Thomas, Ann. Rev. Nucl. Part. Sci. 45, 337 (1995);
R.P. Bickerstaff, A.W. Thomas, J. Phys. G 15, 1523 (1989)
- [3] A. Arima et al., Adv. Nucl. Phys. 18, 1 (1987);
I.S. Towner, Phys. Rep. 155, 263 (1987);
F. Osterfeld, Rev. Mod. Phys. 64, 491 (1992)
- [4] K. Tsushima, D.O. Riska, Nucl. Phys. A 549, 313 (1992)

- [5] K. Kubodera, J. Delorme, M. Rho, Phys. Rev. Lett. 40, 755 (1978);
M. Kirchbach, D.O. Riska, K. Tsushima, Nucl. Phys. A 542, 616 (1992);
I.S. Towner, Nucl. Phys. A 542, 631 (1992)
- [6] J. Morgenstern, Z.-E. Meziani, Phys. Lett. B 515, 269 (2001);
K. Saito, K. Tsushima, A.W. Thomas, Phys. Lett. B 465, 27 (1999)
- [7] S. Malov et al., Phys. Rev. C 62, 057302 (2000)
- [8] S. Dieterich et al., Phys. Lett. B 500, 47 (2001);
R.D. Ransome, Nucl. Phys. A 699, 360c (2002);
S. Strauch et al., Phys. Rev. Lett. 91, 052301 (2003);
S. Strauch (E93-049 Coll.) nucl-ex/0308026.
- [9] J.J. Kelly, Phys. Rev. C 60, 044609 (1999);
J.M. Udias, J.R. Vignote, Phys. Rev. C 62, 034302 (2000);
J.M. Udias et al., Phys. Rev. Lett. 83, 5451 (1999)
- [10] D.H. Lu, A.W. Thomas, K. Tsushima, A.G. Williams, K. Saito, Phys. Lett. B 417, 217 (1998);
D.H. Lu, K. Tsushima, A.W. Thomas, A.G. Williams, K. Saito, Phys. Rev. C 60, 068201 (1999)
- [11] See, e.g., Proceedings of the Workshop on Neutrino - Nucleus Interactions in the Few GeV Region (NuInt01), Tsukuba (Japan), 2001 (Nucl. Phys. B. Proc. Suppl. 112, Issues 1-3 (2002)), see also the web page, <http://neutrino.kek.jp/nuint01/>
- [12] For a review, e.g., A.B. Balantekin, W.C. Haxton, in *Canberra 1998, Frontiers in nuclear physics* 268-350, nucl-th/9903038
- [13] For example, W.M. Alberico, S.M. Bilenky, C. Maieron, Phys. Rep. 358, 227 (2002);
C.J. Horowitz, Hungchong Kim, D.P. Murdock, S. Pollock, Phys. Rev. C 48, 3078 (1993)
- [14] L.B. Auerbach et al., Phys. Rev. C 66, 015501 (2002);
C. Athanassopoulos et al., Phys. Rev. C 56, 2806 (1997);
M. Albert et al., Phys. Rev. C 51, R1065 (1995)
- [15] E. Kolbe, K. Langanke, P. Vogel, Nucl. Phys. A 652, 91 (1999);
C. Volpe et al., Phys. Rev. C 62, 015501 (2000);
A.C. Hayes, I.S. Towner, Phys. Rev. C 61, 044603 (2000);
S.K. Singh, Nimai C. Mukhopadhyay, E. Oset, Phys. Rev. C 57, 2687 (1998);
F. Krmpotić, A. Mariano, A. Samana, Phys. Lett. B 541, 298 (2002);
Y. Umino, J.M. Udias, Phys. Rev. C 52, 3399 (1995);
C. Maieron, M.C. Martinez, J.A. Caballero, J.M. Udias, nucl-th/0303075
- [16] Hungchong Kim, J. Piekarewicz, C.J. Horowitz, Phys. Rev. C 51, 2739 (1995); nucl-th/9502041
- [17] C.J. Horowitz, Hungchong Kim, J. Piekarewicz, Phys. Rev. C 48, 3078 (1993)

- [18] D.H. Lu, A.W. Thomas, K. Tsushima, nucl-th/0112001
- [19] Hungchong Kim, S. Schramm, C.J. Horowitz, Phys. Rev. C 53, 3131 (1996)
- [20] K. Tsushima, D.O. Riska, P.G. Blunden, Nucl. Phys. A 559, 543 (1993)
- [21] W. M. Alberico, T. W. Donnelly, A. Molinari, Nucl. Phys. A 512, 541 (1990)
- [22] P.A.M. Guichon, Phys. Lett. B 200, 235 (1989);
P.A.M. Guichon, K. Saito, E.N. Rodionov, A.W. Thomas, Nucl. Phys. A 601, 349 (1996);
K. Saito, K. Tsushima, A.W. Thomas, Nucl. Phys. A 609, 339 (1996); Phys. Rev. C 55,
2637 (1997)
- [23] For example, see K. Tsushima, hep-ph/0206069, in the Proceedings of Joint
CSSM/JHF/NITP Workshop on Physics at the Japan Hadron Facility, Adelaide (Aus-
tralia), 2002, p. 303;
K. Tsushima, D.H. Lu, W. Melnitchouk, K. Saito, A.W. Thomas, nucl-th/0301078
- [24] A. W. Thomas, Adv. Nucl. Phys. 13, 1 (1984);
G. A. Miller, Int. Rev. Nucl. Phys. 1, 190 (1984)
- [25] K. Saito, Prog. Theor. Phys. 108, 609 (2002);
K. Saito, K. Tsushima, Phys. Lett. B (in press)
- [26] D.H. Lu, A.W. Thomas, A.G. Williams, Phys. Rev. C 57, 2628 (1998)
- [27] A.L. Licht, A. Pagnamenta, Phys. Rev. D 2, 1150 (1970); D 2, 1156 (1970)
- [28] M.J. Musolf, T.W. Donnelly, Nucl. Phys. A 546, 509 (1992)
- [29] T. Kitagaki et al., Phys. Rev. D 28, 436 (1983)
- [30] K. Saito, A.W. Thomas, Phys. Rev. C 51, 2757 (1995)
- [31] R.D. Mckeown, Phys. Rev. Lett. 56, 1452 (1986)
- [32] K.A. Brueckner, Phys. Rev. 110, 587 (1958);
N.M. Hugenholtz, L. Van Hove, Physica 24, 363 (1958)
- [33] A. Hotta, P.J. Ryan, H. Ogino, B. Parker, G.A. Peterson, R.P. Singhal, Phys. Rev. C 30,
87 (1984)
- [34] T. Kuramoto, M. Fukugita, Y. Kohyama, K. Kubodera, Nucl. Phys. A 512, 711 (1990)

Table 1: Calculated total cross sections for $^{12}\text{C}(\nu_\mu, \mu^-)X$. They are calculated using the Fermi gas model with the binding energy E_B , and averaged over the LSND muon neutrino spectrum [14]. For details, see the text.

Notation	Type of calculation	E_B (MeV)	$\langle\sigma\rangle$ in 10^{-40} cm^2
$\langle\sigma(F, G)\rangle$	$m_N, F_{1,2}(Q^2), G_{A,P}(Q^2)$	0	32.5
$\langle\sigma(F^*, G^*)\rangle$	$m_N, F_{1,2}^*(Q^2), G_{A,P}^*(Q^2)$	0	30.0
$\langle\sigma(F, G)\rangle$	$m_N^*, F_{1,2}(Q^2), G_{A,P}(Q^2)$	0	28.4
$\langle\sigma(F^*, G^*)\rangle$	$m_N^*, F_{1,2}^*(Q^2), G_{A,P}^*(Q^2)$	0	26.2
$\langle\sigma(F^*, G)\rangle$	$m_N, F_{1,2}^*(Q^2), G_{A,P}(Q^2)$	0	33.5
$\langle\sigma(F, G^*)\rangle$	$m_N, F_{1,2}(Q^2), G_{A,P}^*(Q^2)$	0	29.1
$\langle\sigma(F, G)\rangle$	$m_N, F_{1,2}(Q^2), G_{A,P}(Q^2)$	20	16.1
$\langle\sigma(F^*, G^*)\rangle$	$m_N, F_{1,2}^*(Q^2), G_{A,P}^*(Q^2)$	20	14.8
$\langle\sigma(F, G)\rangle$	$m_N, F_{1,2}(Q^2), G_{A,P}(Q^2)$	25	13.2
$\langle\sigma(F^*, G^*)\rangle$	$m_N, F_{1,2}^*(Q^2), G_{A,P}^*(Q^2)$	25	12.2
$\langle\sigma(F, G)\rangle$	$m_N, F_{1,2}(Q^2), G_{A,P}(Q^2)$	30	10.7
$\langle\sigma(F^*, G^*)\rangle$	$m_N, F_{1,2}^*(Q^2), G_{A,P}^*(Q^2)$	30	9.9
	Experiment [14] (2002)		$10.6 \pm 0.3 \pm 1.8$
	Experiment [14] (1997)		$11.2 \pm 0.3 \pm 1.8$
	Experiment [14] (1995)		$8.3 \pm 0.7 \pm 1.6$

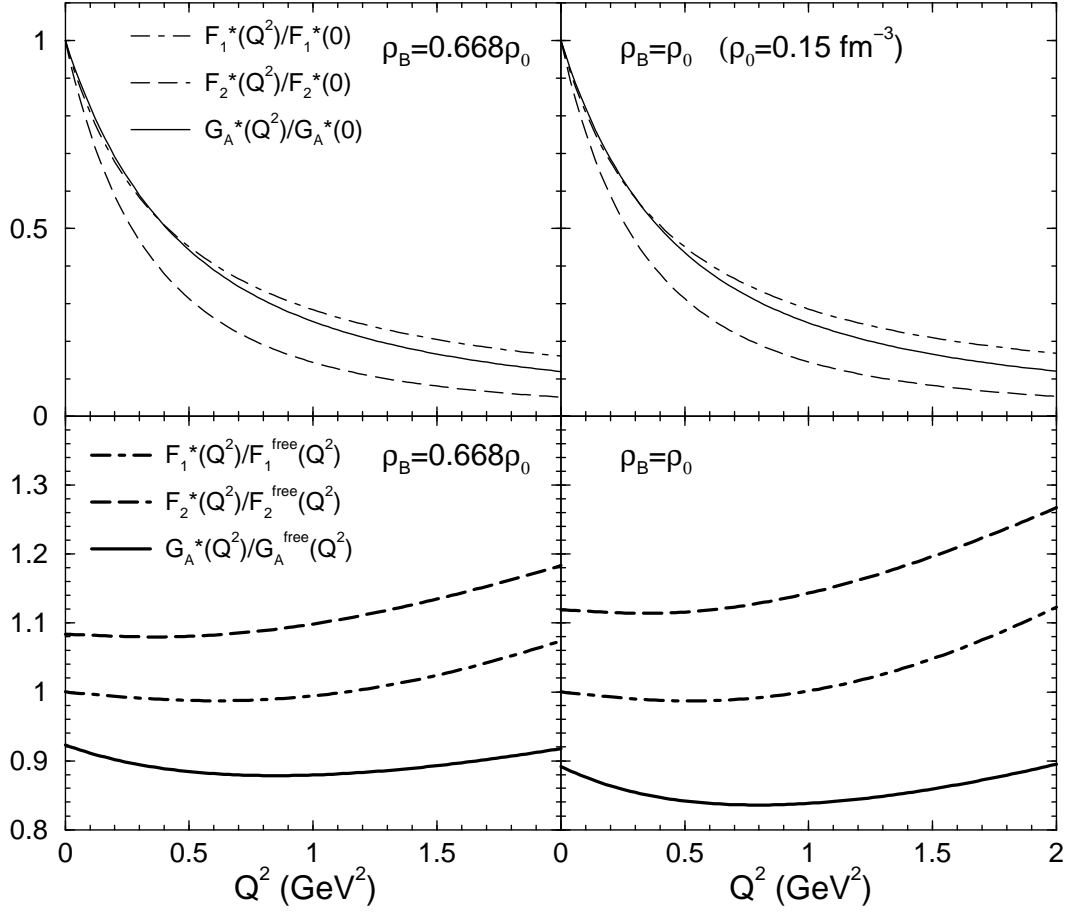


Figure 1: Ratios for the charged-current form factors in nuclear matter calculated in the QMC model, where $0.668\rho_0$ corresponds to the Fermi momentum in ^{12}C , $k_F = 225$ MeV.

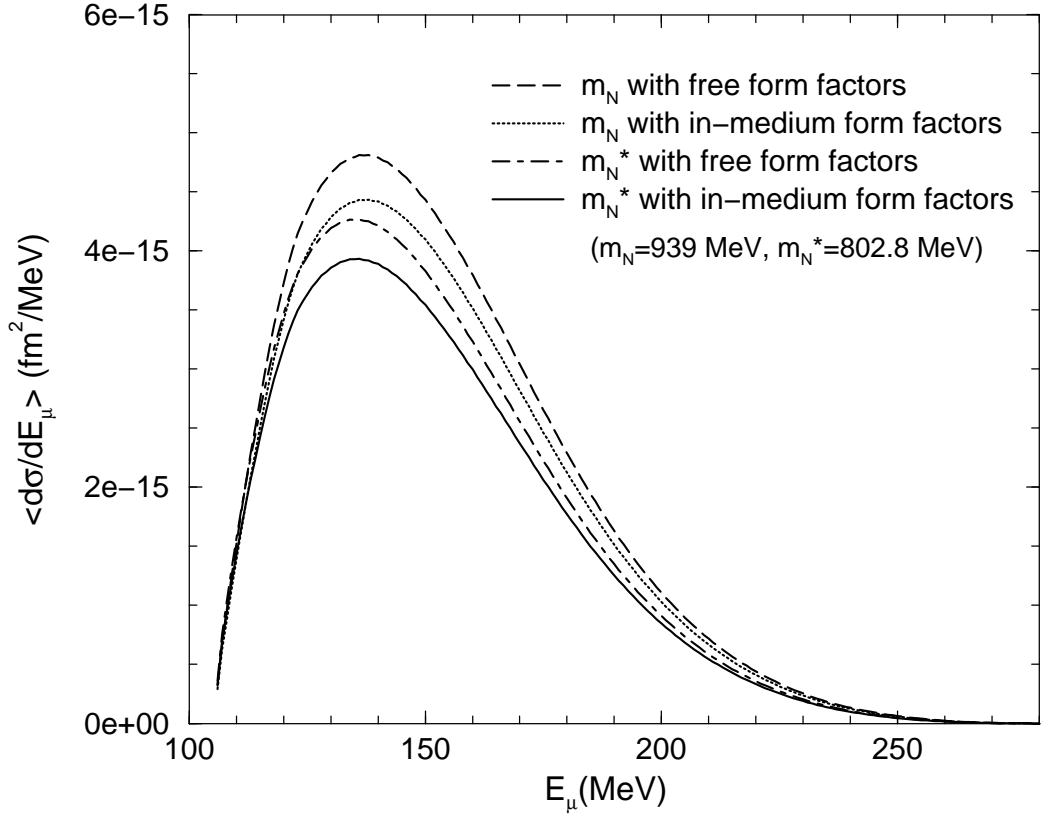


Figure 2: Angle-integrated cross section for the $^{12}\text{C}(\nu_{\mu}, \mu^{-})X$ reaction as a function of the emitted muon energy E_{μ} . They are averaged over the LSND muon neutrino spectrum [14], and calculated using the corresponding bound nucleon form factors for $\rho_B = 0.668\rho_0$ shown in Fig. 1. All calculations are performed with $E_B = 0$.

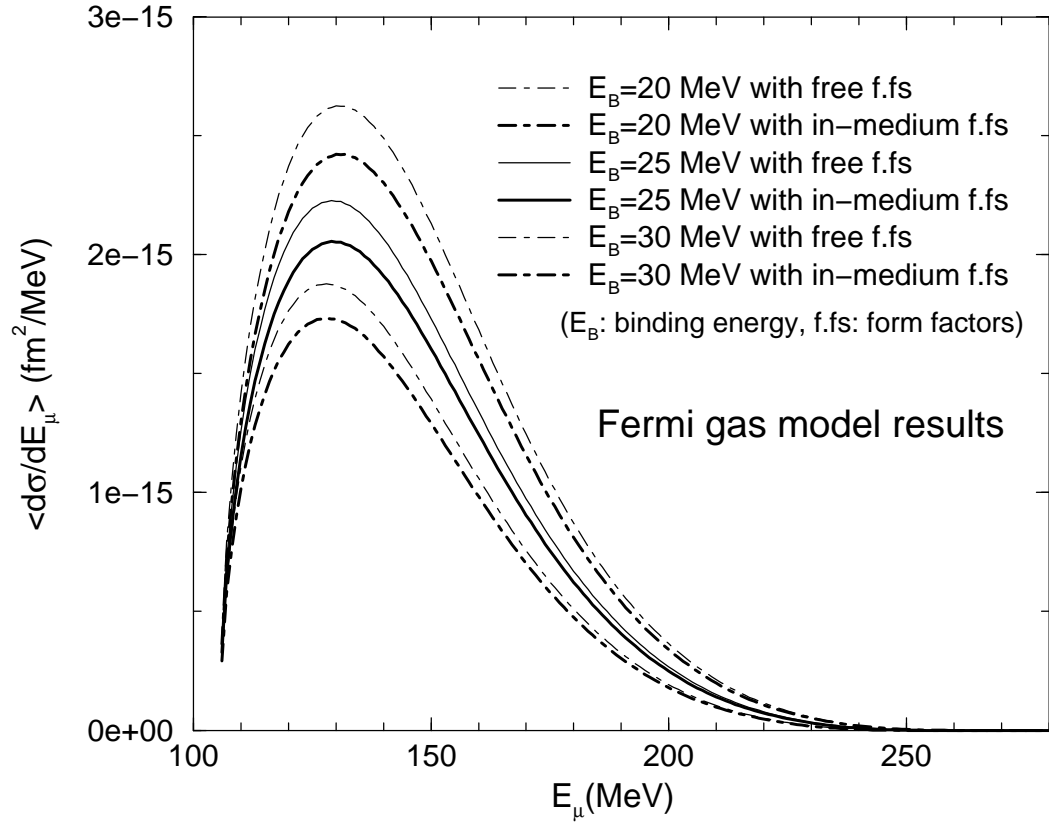


Figure 3: The same as Fig. 2, but using the free nucleon mass $m_N = 939$ MeV for all cases, and for the binding energies, $E_B = 20, 25$ and 30 MeV.